Construction and Building Materials 306 (2021) 124885

Contents lists available at ScienceDirect

Construction and Building Materials

journal homepage: www.elsevier.com/locate/conbuildmat

Performance and radiological implications of using residue from TiO_2 production as a component of coating mortars

Daniel V. Ribeiro [a], Nilson S. Amorim Júnior [b,*], José S. Andrade Neto [c], Diana D. M. Albuquerque [c], Barbara P. Mazzilli [d]

[a] Department of Materials Science and Technology, Federal University of Bahia, Rua Aristides Novis, 02. Federação. 40210-630. Salvador/BA, Brazil
[b] Post-Graduate Program in Civil Engineering (PPEC), Federal University of Bahia, Rua Aristides Novis, 02. Federação. 40210-630. Salvador/BA, Brazil
[c] Laboratory of Testing on Materials Durability (LEDMa), Federal University of Bahia, Rua Aristides Novis, 02. Federação. 40210-630. Salvador/BA, Brazil
[d] Instituto de Pesquisas Energéticas e Nucleares, Av. Prof. Lineu Prestes 2242, CEP 05508000, São Paulo, Brazil

ARTICLE INFO

Keywords:
Coating mortars
Unreacted ore
Applied state
Performance
Radiological implications

ABSTRACT

The objective of this study was to investigate the effect of the addition of residue from the production of TiO_2, namely, unreacted ore waste (UOW), on the properties of coating mortars as well as evaluate its radiological impact. The properties of the mixed cement lime mortars were evaluated after the addition of 5%, 10%, and 15% of UOW, in relation to the cement mass, with respect to the reference mortar. The coating mortars were evaluated for rheology, dynamic elastic modulus, and mechanical strength. Tests in the applied state were performed using panels. From the point of view of radiological protection, the concentration of natural radionuclides in the residue, components of the mortar, and ready mortar were determined. In addition, the concentration of radon in the air and the exposure of dwellers living in a standard room coated with mortar were evaluated. The results obtained indicated that UOW did not compromise the use of coating mortars, presenting no significant effect on the properties of fresh, hardened, and applied states. Although the UOW presented high concentration of radionuclides, mortars with 5%, 10%, and 15% of UOW led to a gamma exposition and indoor radon concentration (average values of 0.20 $mSv.a^{-1}$ and 71 $Bq.m^{-3}$, respectively) below the recommended limits (1 $mSv.a^{-1}$ and 100 $Bq.m^{-3}$). Thus, it is concluded that UOW can be incorporated into coating mortars without presenting risks to the health of users due to radiation exposure.

1. Introduction

The high amount of waste generated by human activity has intensified with the systematization of production processes since the Industrial Revolutions and is considered a significant contemporary problem. Multidisciplinary efforts are required to determine technically and economically viable alternatives for the reuse of these wastes. With growth in production, industries have been emitting an increasing number of gaseous and solid polluting agents, which has become a grave environmental problem owing to the inadequate disposal of these pollutants. Therefore, studies that aim at the viable use of these residues are significant.

According to data from the Brazilian Association of Waste Treatment [1], Brazil generated approximately 33 million tons of industrial waste in 2016, of which 25 million tons were not treated adequately, generating a cost of approximately US$ 172 million per year to the federal government.

The construction industry has the potential to absorb a large portion of solid industrial waste, as it can be used in building materials and elements [2–6]. Cement matrices are highly alkaline and can generally be used in waste packaging because they are inexpensive and accessible. Their high alkalinity inhibits microbiological processes and can incorporate liquid and pasty residues, as they require water for hydration. In addition, they reduce the solubility of several toxic and dangerous organic residues [7].

Several studies have addressed the feasibility of adding various residues in the production of mortars [8–11]. These residues contribute significantly to the workability, deformation, resistance, and permeability of mortars in addition to contributing to the principles related to environmental sustainability in recycling waste, reducing the emission

* Corresponding author.
E-mail addresses: verasribeiro@hotmail.com (D.V. Ribeiro), nilson.amorim18@gmail.com, nilson.santana@ufba.br (N.S. Amorim Júnior), josedasilvaandradeneto@gmail.com (J.S. Andrade Neto), dianadayse@gmail.com (D.D.M. Albuquerque), mazzilli@ipen.br (B.P. Mazzilli).

https://doi.org/10.1016/j.conbuildmat.2021.124885
Received 27 April 2021; Received in revised form 15 August 2021; Accepted 8 September 2021
Available online 23 September 2021

of pollutants, and decreasing the consumption of raw materials [8].

However, few studies have been conducted on using residues from the production of TiO_2, involving the evaluation of photocatalytic performance [12,13], the effect on cement hydration [14–16], and the studies conducted by Potgieter et al. [17], Andrade Neto et al. [18], and Mariani et al. [19], who used TiO_2 residue as a fluxing material for the production of Portland clinker.

The unreacted ore waste (UOW) used in this study is the industrial waste generated in the production of titanium dioxide through the sulfate route at the Tronox Pigmentos do Brasil SA unit in Camaçari/BA, which produces approximately 60,000 tons of TiO_2 annually, generating approximately 30,000 tons of waste.

Titanium dioxide produced using ilmenite as the raw material is classified as a naturally occurring radioactive material (NORM) owing to the presence of natural radionuclides in the ilmenite [16]. During the industrial process, radionuclides are distributed among the products, by-products, and residue, eventually reaching levels that require control by the National Regulatory Agency, Comissão Nacional de Energia Nuclear (CNEN), in Brazil. The residue formed in the production of titanium dioxide, known as UOW, is disposed of in industrial landfills. The deposition of any residue can cause grave environmental hazards; therefore, such practices should comply with the recommendations of the National Environmental Agency. The construction and maintenance of waste deposits is expensive, requires space and continuous monitoring, and presents the risk of environmental contamination. However, the reuse of NORM residues should be considered, provided that this practice does not imply any additional exposure for humans.

Ilmenite has average levels of certain radioactive isotopes such as uranium, thorium, lead, and radium. Among these, uranium and thorium are soluble in sulfuric acid and are used in the sulfation stage. Therefore, it is expected that most of these isotopes are left in the liquor (solution used in the production of TiO_2), implying a low concentration in the UOW. However, radium and lead isotopes have low solubility in sulfuric acid; therefore, it is expected that a large percentage (75% to 95% for radium) will remain in the residue [20].

Albuquerque et al. [21] evaluated the effects of the addition of UOW, from the production of TiO_2 through the sulfate route, on the properties of coating mortars in the hardened and applied states. The authors observed that the addition of up to 15% of the residue did not significantly impact the physical and mechanical properties of the mortars, thereby facilitating the reduction of cement consumption by reusing UOW. Llanes et al. [16] evaluated the use of a resemblant waste and concluded that the residue plays a beneficial role since it reduces the heat of hydration, the final setting time, the expansion, and the linear retraction compared to standard ordinary Portland cement.

Although the use of UOW in mortars is promising, studies on the impact of the residue on the other properties of the mortar, associated with its workability (rheology) and the evaluation of the internal and external exposure of individuals living in a standard room covered with such mortar, are necessary to enable its use.

Gázquez et al. [22] studied a residue formed during the production of titanium dioxide through the sulfate route with characteristics similar to those of the UOW used in the present work and obtained a ^{228}Ra concentration of 2.6 Bq/g, which is, according to the authors, 100 times higher than the concentration determined in typical soils. The authors also obtained ^{226}Ra concentrations of 0.82 Bq/g and lower concentrations of uranium isotopes (0.210 Bq/g for ^{238}U and 0.240 Bq/g for ^{234}U) and thorium isotopes (0.350 Bq/g for ^{232}Th, 0.045 Bq/g for ^{230}Th, and 0.680 Bq/g for ^{228}Th).

Llanes et al. [16] carried out a radiological characterization of cementitious matrix containing different contents (up to 10%) of ilmenite mud (a waste from TiO_2 production, similar to UOW). The authors found that the cementitious matrix immobilized the radionuclides present in the waste, and the radionuclides contents present in the liquid fractions extracted from the cementitious matrix (containing the ilmenite mud) were negligible [16]. However, it is stressed that UOW presents some differences when compared to the ilmenite mud used by Llanes et al. [16], as the ilmenite mud is not neutralized by hydrated lime. Besides that, there are variations in the ilmenite and in the concentration of sulphuric acid used in the process. Furthermore, Llanes et al. [16] did not evaluate the concentration of radon in the air and exposure to individuals living in a room covered with the mortar containing UOW.

The radioactivity of the residue can become an obstacle for certain applications of products containing UOW, such as coating mortars, in direct contact with users. Thus, this paper describes a scientific contribution to characterize and test the effect of adding a little-known and little-studied residue in coating mortars through the analyses of the fresh (rheology), hardened (flexural and compressive strengths, dynamic elastic modulus, apparent porosity, and density), and "applied" (tensile bond strength/pull-off and absorption by the Karsten pipe) states.

Furthermore, to evaluate the possibility of using this residue in the production of mortar, from the point of view of radiological protection, the concentrations of natural radionuclides in the residue, components of the mortar, and mortar with proportions of UOW of 5%, 10%, and 15% were determined. In addition, the concentration of radon in the air and exposure to individuals living in a standard room covered with mortar were evaluated.

2. Materials and methods

2.1. Materials

The UOW used in this study was generated and supplied by Tronox Pigmentos do Brasil SA and collected according to the waste sampling methodology specified in NBR 10007 [23]. UOW is generated during the processing of a mixture of ilmenite ($FeO.TiO_2$) and titanium slag to produce the TiO_2 pigment. In this process, this mixture goes through two stages until the generation of UOW: i) in the sulfation stage, ilmenite and titanium slag are attacked by sulfuric acid, and ii) in the neutralization stage, the mixture is filtered and the unreacted part (solid material) is neutralized with calcium hydroxide [$Ca(OH)_2$], producing the UOW. The TiO_2 production process and the generation of the unreacted ore are depicted in Fig. 1.

After collecting the UOW batches, a beneficiation process was carried out, consisting of drying in an oven at a temperature of 105 ± 5 °C for 24 h, grinding in a QUIMIS horizontal rotary mill, model Q298, containing ceramic balls for 30 min, followed by sieving through a mesh with a #75 μm opening.

For the production of mortars, white Portland cement, produced by CEMEX TOLTECA, sand from a deposit and commercially available in the metropolitan region of Salvador, hydrated lime (CH-II), and potable water were used.

2.2. Methods

2.2.1. Mortar dosage and cast

The coating mortars were produced using a 1:1:5:1.3 ratio for the ingredients (white Portland cement:hydrated lime:sand:water) in bulk using the Selmo Dosing Method [24], with the addition of 5%, 10%, and 15% of UOW with respect to the cement mass. Table 1 lists the material consumed per cubic meter of the mortar produced. It was observed that the addition of the residue reduced the amounts of cement, lime, sand, and water used.

Subsequently, the mortars were mixed in a bench-top mortar mixer, planetary type, according to the procedure recommended by NBR 13276 [25].

2.2.2. Characterization of raw materials

Initially, tests were carried out to characterize the physical and chemical properties of the raw materials. The physical characterization of White Portland cement, hydrated lime, and UOW were performed

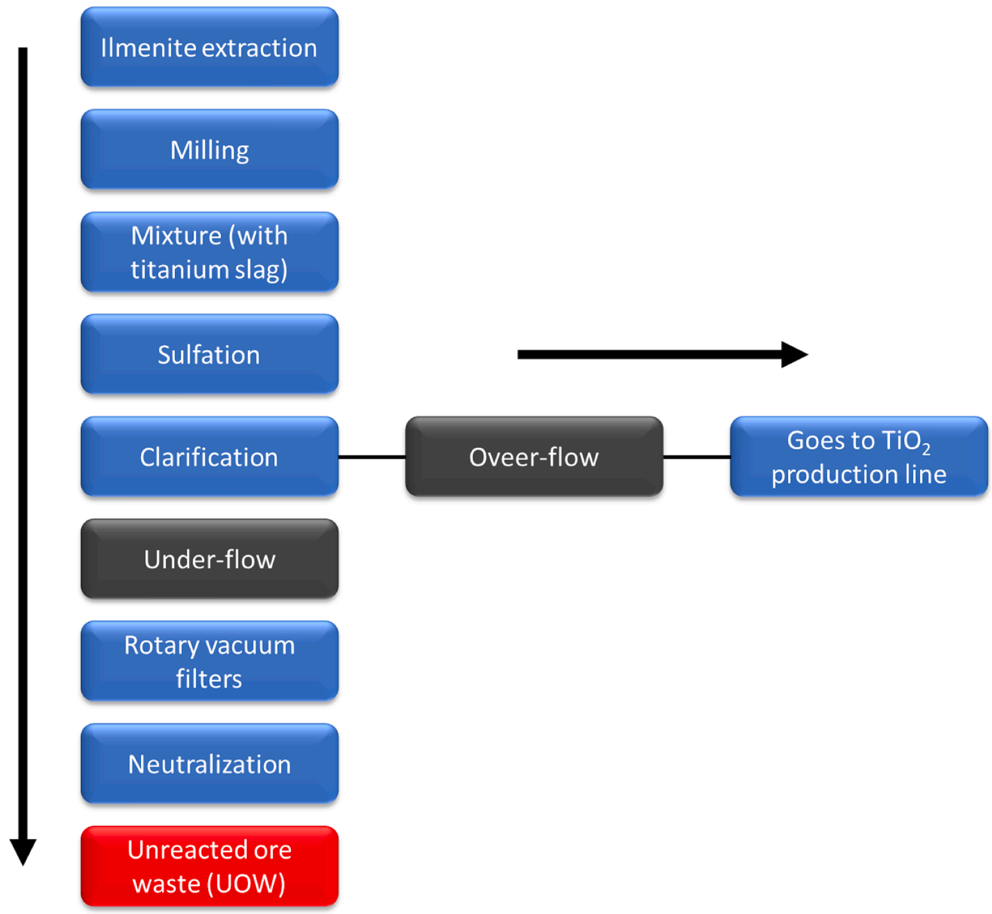

Fig. 1. TiO_2 production process and generation of unreacted ore (UOW) at Tronox Pigmentos.

Table 1
Consumption of raw materials for the production of one cubic meter of mortar.

Mixture	Cement (kg)	Lime (kg)	Sand (kg)	Water (kg)	UOW (kg)
REF	255.28	255.28	1276.42	331.87	0.00
5% UOW	254.22	254.22	1271.12	330.49	12.71
10% UOW	253.17	253.17	1265.86	329.12	25.32
15% UOW	252.13	252.13	1260.65	327.77	37.82

using a helium gas pycnometer (Micromeritics AccuPyc II 1340) for specific gravity, a semi-automatic air permeability instrument (ACMEL, model BSA1) for the Blaine surface area, and a laser granulometer (CILAS 1180) for particle size distribution.

The fine aggregate (sand) was characterized in terms of particle size distribution, fineness modulus, and maximum diameter by mechanical sieving according to the method described in NBR NM 248 [26]. The specific gravity of the sand was determined according to the method described in NBR NM 52 [27].

The chemical composition of UOW, in the form of oxides, was determined through X-ray fluorescence (XRF) using Bruker's S2 Ranger equipment. X-ray diffraction (XRD) was used to identify its mineralogical composition. For this, a D2 Phaser Bruker diffractometer was used with a copper target tube (Kα radiation with a wavelength of 1.54060 Å) at 30 kV and 10 mA, without a filter system, and with a secondary monochromator. The diffraction spectra were obtained in the range of 2θ from 5° to 80° using continuous scanning at 0.004°/s for all the analyses. The phases present in the samples were subsequently identified using the computer program DIFFRAC plus-EVA, with a database centered on the COD system (Crystallography Open Database), and quantified using the Rietveld method, employing the computer program TOPAS and the Crystallographic Information File (CIF). All the tests performed to characterize the raw materials were performed in triplicate measurement.

2.2.3. *Characterization of fresh state*

The mortar spread on a table (flow table) was determined according to the procedures described in NBR 13276 [25]. To achieve this, a Contenco automatic consistency table (model I-3019-B) was used. As the flow-table test is a single-point test, insufficient for describing the complex rheological behavior of mortars [28,29], the squeeze-flow test was also carried out, according to the method described in NBR 15839 [30].

The squeeze-flow test was carried out on the mortars after 15 min of mixing them with a displacement speed of 0.1 mm/s, in a universal INSTRON testing machine, with displacement control and a 2 kN load cell. The tests were repeated three times for each mixture, and the average results are presented in this paper.

2.2.4. *Characterization of hardened state*

For the characterization of the mortar in the hardened state, three prismatic specimens (4 cm × 4 cm × 16 cm) were molded for each mixture using three specimens of each age to determine the flexural strength. After fracture, these specimens gave rise to six specimens, which were used to determine the compressive strength. The specimens were demolded after 24 h and, thereafter, immersed in water saturated with lime. The immersed cure was maintained until the test was completed.

The tests were carried out to determine the flexural and compressive strengths of the mortars at 3, 7, and 28 days, following the procedure described in NBR 13279 [31]. For this purpose, a Contenco servo-controlled machine (model HD-120 T) with a load capacity of 120 ton-force was used. To determine the flexural strength, the specimens were placed in the load device for flexural tests at three points (with a distance of 120 mm between the supports) and loaded until rupture at a rate of 50 N/s. The two halves obtained in the flexural rupture of each specimen were then positioned in the loading device for compressive tests with the aid of square steel plates (40 mm edge) and loaded until rupture at a rate of 500 N/s.

To determine the apparent porosity and density of the mortar samples, three specimens were used for each mix and tested at 28 days according to the method described in NBR 9778 [32]. The dynamic elastic modulus at 28 days was determined using PROCEQ's ultrasonic wave emitting equipment, model Pundit LAB+, according to the procedure described in NBR 15630 [33] using three samples of each mixture.

2.2.5. *Characterization of applied state*

Finally, to assess the impact of the addition of the UOW on the applied state, masonry panels of dimensions 60 cm × 60 cm were constructed. This masonry was applied with a 1:3 (cement:sand) layer of roughcast and cured for 3 days with water spray. Thereafter, the produced coating mortars (reference and those containing different UOW contents) were applied at an average thickness of 30 mm and cured with water spray for 7 days. The construction of the panels and the execution of the coating were carried out by a civil construction professional to better simulate the application conditions.

To determine the tensile bond strengths, at 28 days, the procedure described in NBR 13528 [34] was used, and the test was performed on 12 specimens of each mixture. To assess the water absorption/permeability of mortars under low pressure, at 72 days, the Karsten pipe was used in a method known as the "pipe method," proposed by the Center Scientifique et Technique de la Construction (CSTC) of Belgium [35], the test being performed in triplicate.

2.2.6. *Radiological characterization of mortar components and applied mortar*

For the radiological evaluation of the UOW residue in the production of mortar, the initial concentration of natural radionuclides was

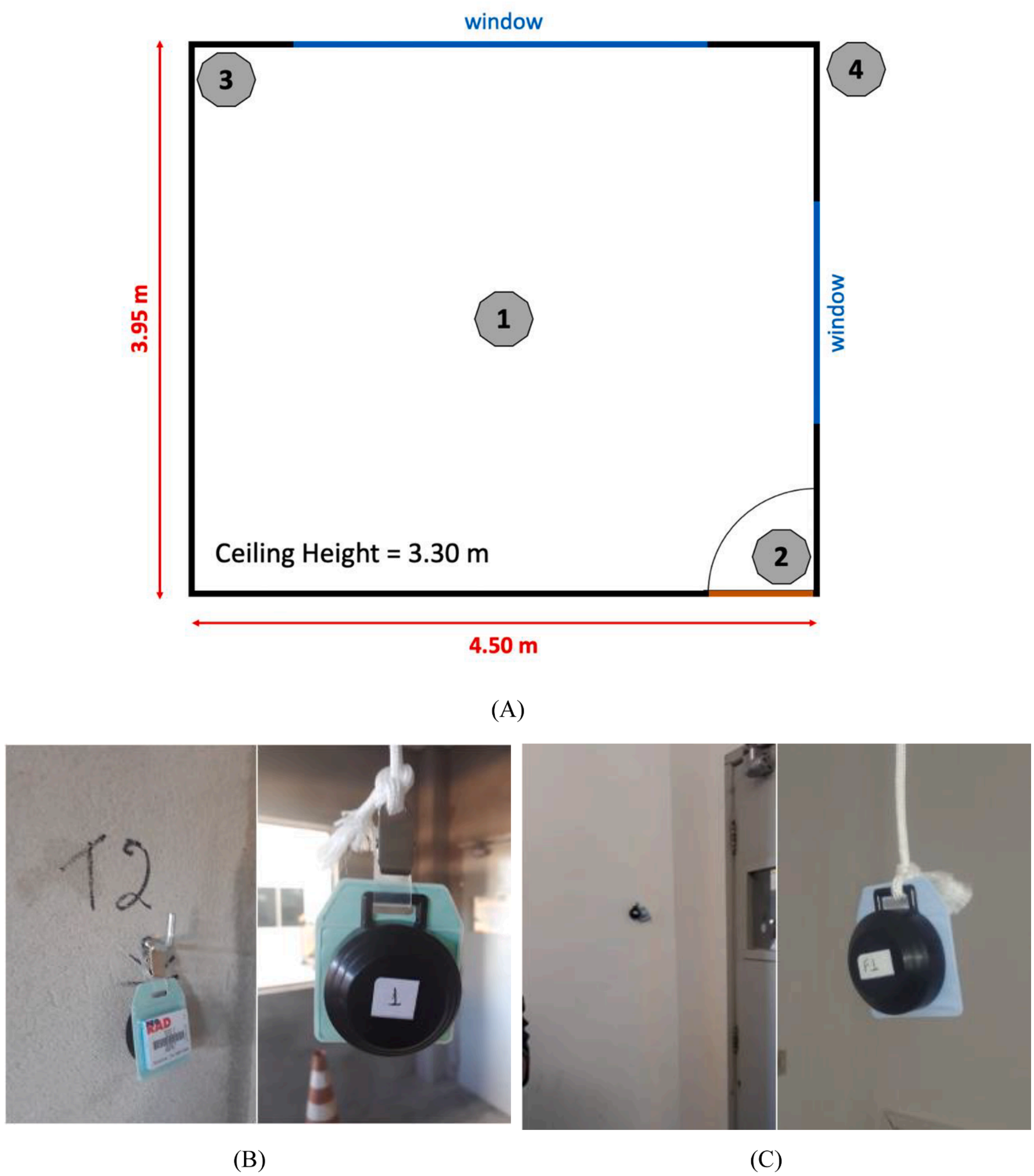

Fig. 2. (A) Dosimeter distribution in the test room. CR-39 and TLD dosimeters installed: (B) before and (C) after applying the mortar containing UOW.

determined in the samples of UOW, lime, sand, cement, and in the prepared mortar with various proportions of the UOW residue. The concentrations of Ra-226, Ra-228, Pb-210, and K-40 were measured through gamma-ray spectrometry using a hyperpure germanium detector (HPGe Canberra, GX4020) with a relative efficiency of 47.2% and a resolution of 1.76 keV at the 1332.40-keV photopeak of ^{60}Co, with the associated electronics coupled to a microcomputer.

To determine the concentrations of U-238 and Th-232, the neutron activation analysis technique was used, which consists of irradiating samples and certified reference standards, in a neutron flow of 10^{12}n.cm^{-2}s^{-1}, in the nuclear reactor IEA-R1 of the Nuclear Energy Research Institute (IPEN) and measuring the gamma activity induced in a hyperpure germanium detector.

To evaluate the dose by external and internal exposure for individuals of the public owing to the applied mortar, a standard room covered with mortar consisting of 15% UOW was used (Fig. 2). In this room, the radon concentration in the air was obtained by employing the passive detection method using solid-state nuclear track detectors (CR-39) in diffusion chambers, and the gamma external exposure was determined using a thermoluminescent dosimeter (TLD).

Four (04) CR-39 detectors and TLD dosimeters were installed: one near the entrance door, the second in the center of the room, the third in the direction diagonally opposite to the first two, and finally the last one was placed outside the room, as illustrated in Fig. 2A. The detectors were installed before applying the mortar to determine the background radiation levels of the site (Fig. 2B) at a height compatible with the respiratory tract of a standing adult. The CR-39 and TLD detectors were exposed for 3 months and removed thereafter for data acquisition. After this period, the mortar was applied to the entire sidewall of the room, and the sensors were replaced in the same position as indicated in Fig. 2A, remaining in the testing position for 3 months (Fig. 2C) and later being removed for data acquisition.

Because the distribution of natural radionuclides in building materials is not uniform, a common radiological index, referred to as the radium equivalent activity (Ra_{eq}), is introduced to represent the specific radioactivity levels of ^{226}Ra, ^{232}Th, and ^{40}K. This index considers the associated radiation hazards. The radium equivalent activity was calculated based on the estimation that 1 Bq•kg^{-1} of ^{226}Ra, 0.7 Bq•kg^{-1} of ^{232}Th, and 13 Bq•kg^{-1} of ^{40}K produced the same dose rate owing to the external gamma irradiation. The radium equivalent activity $C_{Ra,eq}$ (in Bq.kg^{-1}) was determined using Equation (1):

$$C_{Ra,eq} = C_{Ra} + 1.43C_{Th} + 0.077C_K \quad (1)$$

where C_{Ra}, C_{Th}, and C_K denote the activity concentrations (in Bq.kg^{-1}) of ^{226}Ra, ^{232}Th, and ^{40}K, respectively.

The use of building materials with $C_{Ra,eq}$ exceeding 370 Bq•kg^{-1} is not recommended to avoid additional risks from external exposure. The activity concentration index (I) was calculated as recommended by the European Commission (EC, 1999) [36] according to Equation (2):

$$I = \frac{C_{Ra}}{300} + \frac{C_{Th}}{200} + \frac{C_k}{3000} \quad (2)$$

According to the recommendation, the activity concentration index I should be less than 1 to ensure that the dose received by individuals exposed to gamma radiation present in construction materials does not exceed the value of 1 mSv/a.

2.2.7. *Statistical analysis of results*

The results obtained for the fresh state and all the results of characterization in the hardened and applied states were statistically analyzed using a single-factor ANOVA test, with the level of significance, $\alpha = 0.05$.

3. Results and discussion

3.1. *Characterization of materials*

Table 2 and Fig. 3 indicate the results of the physical characterization and the particle size distribution curves, respectively, of the raw materials used. The results obtained indicate the high fineness of the UOW, which presented an intermediate particle size distribution curve for cement and lime.

Based on the results of the chemical characterization of the UOW (Table 3), the high content of titanium dioxide was attributed to the raw materials (ilmenite and titanium slag) used in the production process. The presence of calcium oxide (CaO) and sulfur trioxide (SO_3) can be attributed to stages in the UOW generation process (neutralization and sulfation, respectively). Iron oxide (Fe_2O_3) is produced by the oxidation of iron present in ilmenite. Silica (SiO_2) is probably associated with contamination (sand) at the time of collection and/or storage of waste. The other compounds are associated with impurities contained in the UOW.

Figure 4 presents the X-ray diffractogram of the UOW, identifying the crystalline phases. Peaks were observed in the crystalline phases of titanium dioxide in the anatase (TiO_2) and rutile (TiO_2) forms, arising from the nondissolution of the raw material (ilmenite and titanium slag) in sulfuric acid. Anhydrite ($CaSO_4$) is probably the result of reactions between sulfuric acid, used in the sulfation stage, and calcium hydroxide, which is added to the residue to neutralize its pH and, thus, facilitate its disposal. Ilmenite (Fe_2TiO_5) originates from the ilmenite ore, and Armalcolite ($MgTi_2O_5$) may be associated with titanium slag. Calcite ($CaCO_3$) is probably the result of the carbonation reaction between calcium hydroxide [$Ca(OH)_2$] and atmospheric carbon dioxide (CO_2) and quartz (SiO_2), zircon ($ZrSiO_4$), and hematite (Fe_2O_3) owing to impurities and/or contamination in the raw materials.

3.2. *Characterization of fresh mortar*

Figure 5 presents the results of the mortar spread on the table, obtained through the consistency table (flow table). A reduction was noted in the spread with the incorporation of the UOW. The reference mortar indicated a spread diameter of 248 mm, whereas mortars with 5%, 10%, and 15% of UOW had diameters of 244, 240, and 232 mm, respectively. The reduction in the spread diameter as a function of the UOW content, although low (approximately 6%), was statistically significant, as can be seen in Table 4.

The flow table is a single-point test: a method that measures the flow of matter through a single shear rate and, therefore, is unable to fully characterize the mortars, as the results do not distinguish among the contributions of the primary rheological parameters such as viscosity and shear rate [37]. Thus, squeeze-flow tests were performed to better analyze the rheological performance of the mortars containing UOW.

Figure 6 depicts the curves obtained in the squeeze-flow test (load as a function of displacement) for reference mortars and with levels of 5%, 10%, and 15% of UOW obtained 15 min after mixing. It should be noted that stage I, referring to the regime of elastic deformation, is quite short

Table 2
Physical properties of white cement, lime, UOW, and sand used.

Properties	White cement	Lime	UOW	Sand
Specific gravity (g/cm^3)	3.05 ± 0.01	2.40 ± 0.01	3.06 ± 0.01	2.67 ± 0.02
Blaine surface area (cm^2/g)	3715 ± 39	5304 ± 205	3681 ± 481	–
D_{50} (μm)	12	29	22	260
Maximum diameter (mm)	–	–	–	1.18
Fineness modulus	–	–	–	1.32

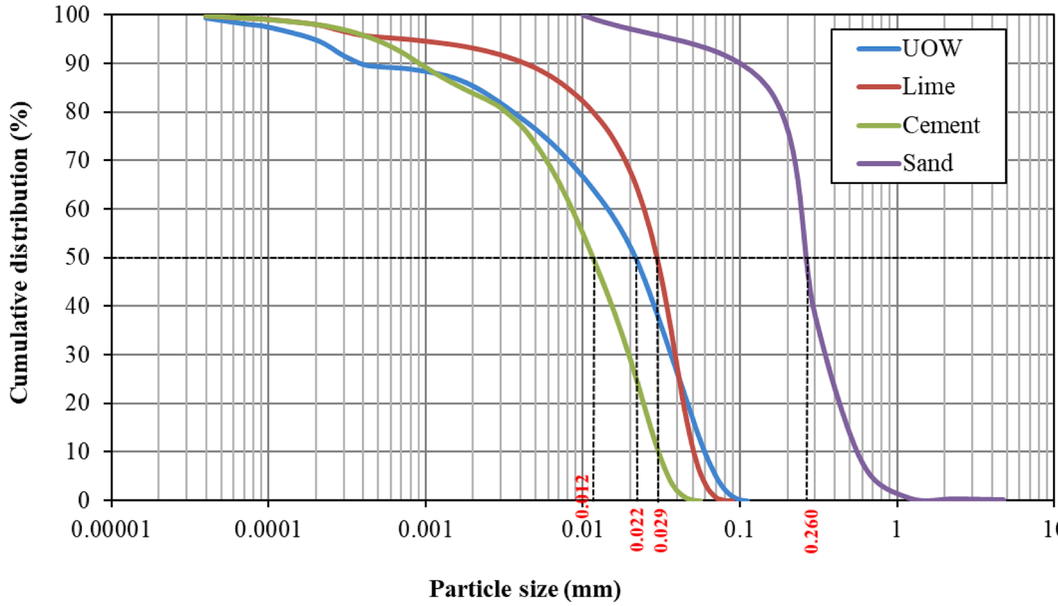

Fig. 3. Particle size distribution curves of the raw materials.

Table 3
Chemical composition, in oxides, of UOW, determined by X-ray fluorescence spectrometry.

Oxides	TiO_2	SiO_2	CaO	SO_3	Fe_2O_3	Na_2O	Al_2O_3	MgO	ZrO_2	LOI*
Content (%)	43.40	14.70	13.20	10.00	7.61	3.04	2.56	1.49	1.47	2,53

* Loss on ignition at 1000 °C.

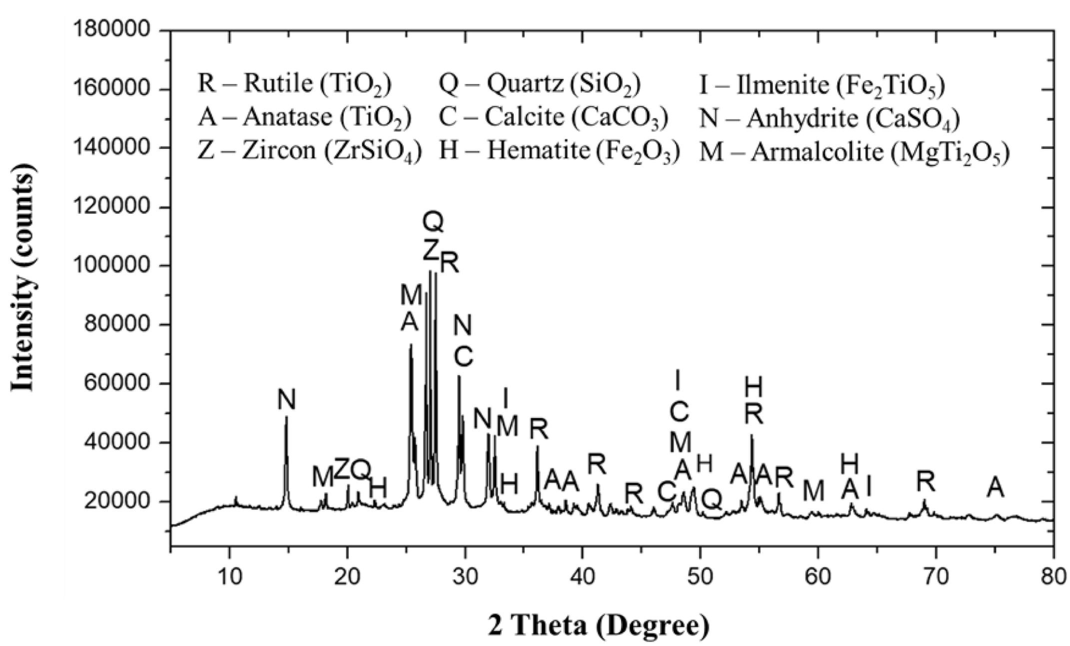

Fig. 4. X-ray diffractogram of the UOW, with identification of crystalline phases.

and imperceptible within the scale of the graph. Stage II, referring to large deformations with low increase in load, and stage III, referring to small deformations with a large increase in load, are more noticeable.

As illustrated in Fig. 6, a reduction in the displacement was obtained at the end of the test, with increase in the amount of added UOW, indicating that the addition of the residue is responsible for a reduction in the plasticity of the mortars. The addition of the residue leads to the reduction of the plastic deformation stage and viscous flow (stage II), thereby requiring higher loads for the same displacement, which makes it difficult to apply the mortar to the building site [29].

The flow-table and squeeze-flow tests indicated the loss of plasticity of the mortars with an increase in the amount of UOW added. The observed performance is attributed, in part, to the higher content of solid particles in the mixtures as well as to the fact that the UOW

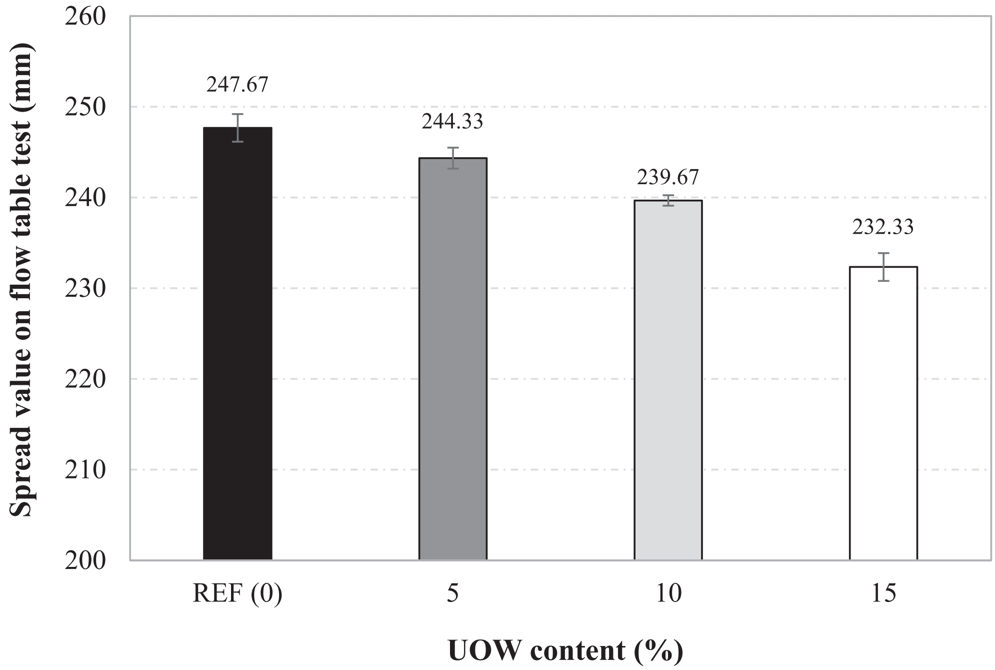

Fig. 5. Spread value on flow table test as a function of UOW addition content.

Table 4
ANOVA statistical analysis of the results testing the influence of the addition of UOW on the physical–mechanical properties of mortars.

Properties	Sum of squares	Degrees of freedom	Mean square	F value	P value	Fc critical	Significant effect
Spread on table	397.34	3	132.44	83.65	0.0000	4.07	Yes
Density	0.00	3	0.00	2.41	0.1425	4.07	Not
Porosity	0.27	3	0.09	1.56	0.2739	4.07	Not
Dynamic elastic modulus	77140.80	3	25713.60	0.85	0.5082	4.07	Not
Flexural strength – 3 days	2.66	3	0.89	3.59	0.0658	4.07	Not
Flexural strength – 7 days	8.57	3	2.85	38.37	0.0000	4.07	Yes
Flexural strength – 28 days	1.60	3	0.53	0.79	0.5333	4.07	Not
Compressive strength – 3 days	3.40	3	1.13	1.26	0.3505	4.07	Not
Compressive strength – 7 days	4.37	3	1.46	2.62	0.1874	4.07	Not
Compressive strength – 28 days	5.71	3	1.90	1.55	0.2756	4.07	Not

Note: If $P < 5\%$, and $Fc < F$ value, the result is significant, considering the 95% confidence interval.

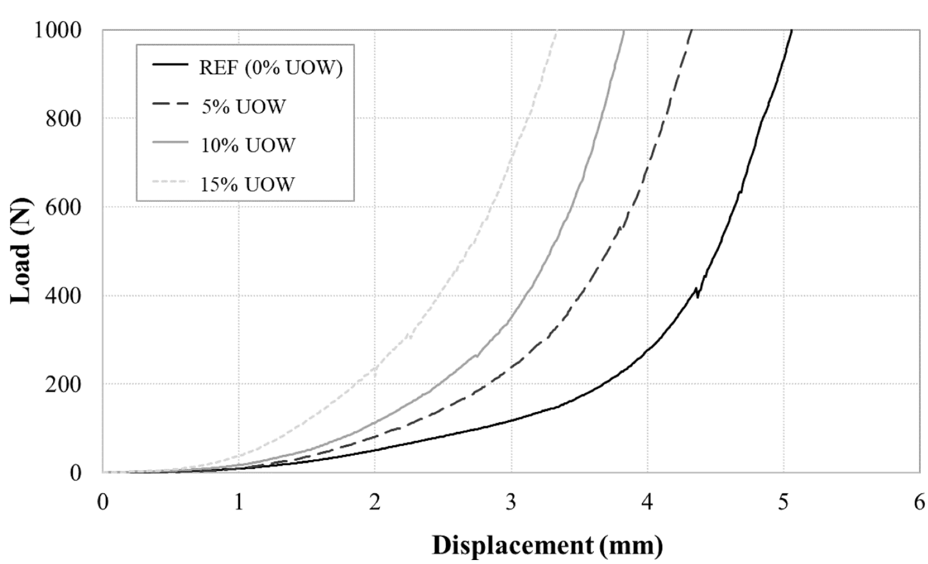

Fig. 6. Load curves as a function of displacement obtained by squeeze-flow for reference mortars (REF) and with levels of 5%, 10%, and 15% of UOW.

particles act as a barrier to the flow of fluid around them, disturbing the flow lines, which no longer appear parallel and start to form curves, thereby increasing the viscosity of the mixture [38].

In addition, owing to the high fineness of the residue, as evidenced by the results of the specific Blaine surface area (Table 2) and granulometry (Fig. 3), a portion of the water is adsorbed by the UOW particles, thereby reducing the amount of water available for the mortar [39–41]. Finally, fine particles have a natural tendency to agglomerate in an aqueous medium because of the capillary and van der Waals forces [42,43]. These agglomerates increase the viscosity and yield stress of the mortar, thereby reducing the plasticity of the mixture [43,44].

3.3. Characterization of hardened state

The results of apparent porosity and density of the mortars containing different contents of UOW at 28 days of age are presented in Fig. 7A and B, respectively, and the statistical analysis of these results using the ANOVA method is presented in Table 4. There was no statistically significant variation in the apparent porosity and density values caused by the addition of UOW.

The addition of UOW containing particles of varying sizes and with a Blaine surface area close to that of cement could promote an increase in the mortar compactness owing to better packing of the particles, leading to a reduction in the porosity. In contrast, the loss of plasticity caused by the addition of the residue, observed in the flow-table and squeeze-flow tests, generated difficulties in the molding and densification, which may cause an increase in the porosity. Further, the reduction in cement consumption also favors a reduction in the density and increase in the porosity of the matrix. Thus, with the joint occurrence of these effects, there was no significant difference in the apparent porosity and density of the mortars.

The values of the dynamic modulus obtained for the studied mortars are indicated in Fig. 8, and the results of statistical analysis using the ANOVA method are presented in Table 4.

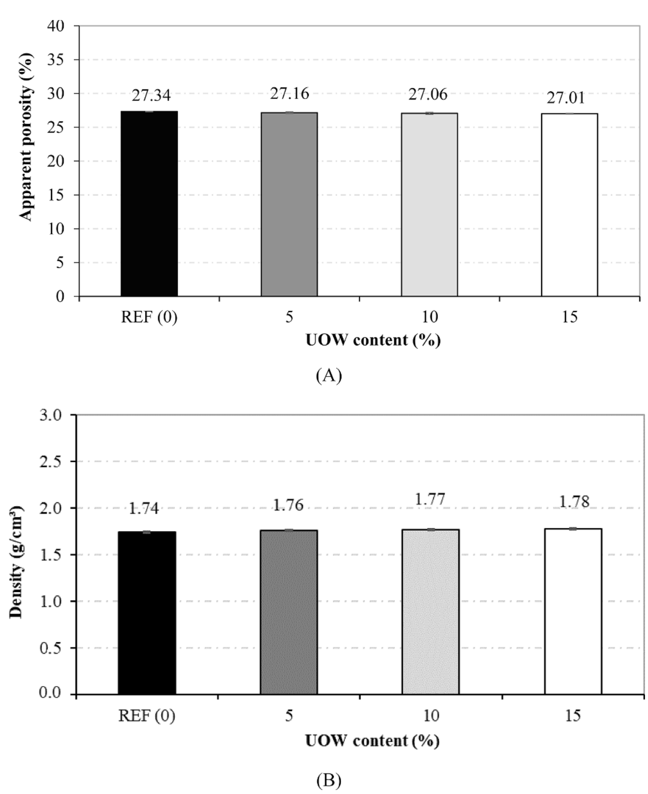

Fig. 7. (A) Apparent porosity and (B) density of mortar samples as a function of UOW content, at 28 days of age.

When calculating the dynamic elastic modulus, the ultrasonic propagation speed in the mortar samples was considered. The time required for the pulse to pass through the sample depends on the pores and/or microcracks, which deviate the pulse and decrease its speed [45]. Thus, a higher ultrasonic propagation speed will result in a higher dynamic modulus value, thereby indicating a smaller number of voids and microcracks and, consequently, higher resistance [46]. As presented in Table 4, no significant differences were observed in the elastic modulus as a function of the added UOW content, corroborating the apparent porosity and density results presented in Fig. 7.

Figures 9 and 10 present the results obtained in the tests of flexural strength and compressive strength, respectively, of mortars with various levels of UOW, depending on the ages of the tested specimens. Based on the statistical analysis using the ANOVA method with $\alpha = 0.05$ (Table 4), it was observed that, in general, the addition of the residue in the mixtures did not promote significant changes in the flexural and compressive strengths, which is in accordance with the results of density, porosity, and dynamic elastic modulus.

As discussed in the results of the mortar porosity, this performance is attributed to the overlap of the filler effect (favorable to the increase in mechanical strength) as well as the loss of workability and reduction of the cement content (disadvantageous to the mechanical strength) with the addition of increasing amounts of UOW. Moreover, it is essential to highlight the fact that the UOW does not harm the basic properties of the coating mortar when added up to levels of 15% because, in addition to reducing the consumption of other materials (cement, lime, and sand) and providing an adequate destination to the UOW, the mortars produced with this residue demonstrated satisfactory photocatalytic capacity, as verified in other studies [13].

3.4. Characterization of applied state

In the third evaluation step, the performance of the coating mortars when applied to the masonry panels was analyzed. The tensile bond strengths of the reference and UOW-containing mortar samples are depicted in Fig. 11, and the statistical analysis of these results using the ANOVA method is presented in Table 5. It is observed that there was no significant variation between the results, with all the mortars produced indicating an adhesion resistance higher than the minimum specified by NBR 13528 [34], that is 0.3 MPa, at 28 days. Thus, we observe that the UOW does not affect the adhesion of the mortars, which is one of its most significant characteristics.

Figure 12 presents the results of water absorption under low pressure and the evolution of these results over 60 min, characterizing the permeability of the coating mortar. The results indicate that all the mortars (reference and containing different levels of UOW) illustrated water absorption below 4 mL during the first 15 min, a result considered positive for coating mortars [47], with statistically insignificant variations among the different levels of addition, according to the ANOVA analysis presented in Table 5.

As discussed for the results of rheology, density, porosity, and mechanical strength, similar results determined in the low-pressure absorption test (for permeability) using the Karsten pipe are attributed to the overlap of several effects when incorporating the residue. The filler effect and better packing of particles with the addition of UOW, with particles of different sizes, favors the reduction of mortar permeability. However, the reduction in cement consumption and the loss of plasticity, with the addition of the residue, generates an opposite effect, favoring an increase in permeability. Thus, globally, no significant differences in mortar permeability were observed with the addition of UOW.

3.5. Radiological characterization and exposure assessment owing to use of waste as mortar component

Table 6 lists the concentrations of natural radionuclides in UOW

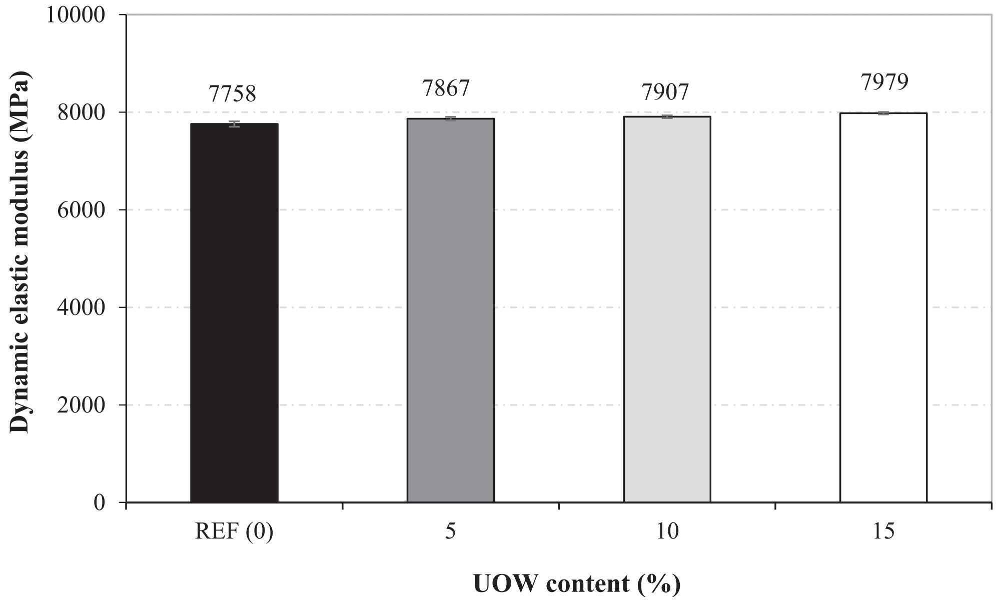

Fig. 8. Dynamic elastic modulus of mortars, at 28 days, as a function of UOW content.

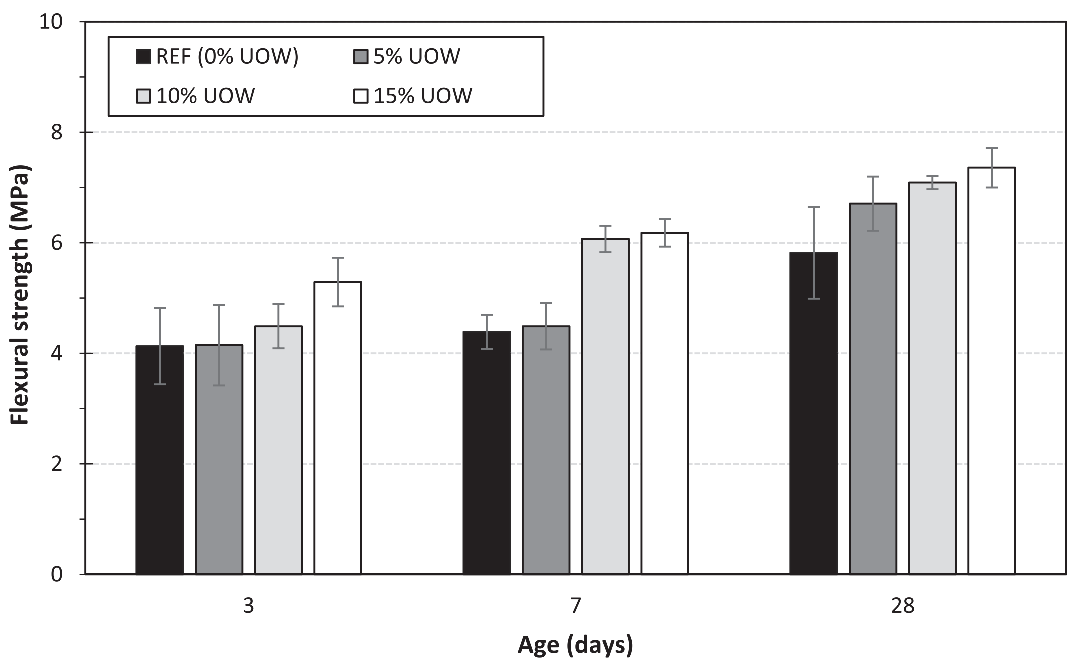

Fig. 9. Flexural strength of mortars with different levels of UOW, as a function of time.

samples, conventional materials used in the preparation of the mortar, and mortar samples after mixing in various proportions of UOW (5%, 10%, and 15%). The values represent the average obtained from the analysis of five different samples. The table also lists the values obtained for $C_{Ra,eq}$ and I.

The raw material, ilmenite, used at Tronox Pigmentos do Brasil SA presents a concentration of radionuclides from the natural series of radioactive decay of U and Th in secular equilibrium (84 ± 6 $Bq.kg^{-1}$ of ^{238}U, 22 ± 1 $Bq.kg^{-1}$ of ^{226}Ra, 37 ± 4 $Bq.kg^{-1}$ of ^{232}Th, and 38 ± 2 $Bq.kg^{-1}$ of ^{228}Ra). During processing through the sulfate route, radionuclides are redistributed according to their chemical properties among the products, by-products, and waste. As U and Th are soluble in sulfuric acid, which used in the sulfation stage, most of these isotopes are concentrated in the liquor, leaving a low concentration in the UOW.

In contrast, lead and radium isotopes can precipitate in the presence of sulfuric acid because their sulfates are highly insoluble and, therefore, tend to be concentrated in the residue. UOW is considered the most critical by-product of the process, with high concentrations of all the radionuclides; in particular, radium isotopes (1103 ± 115 $Bq.kg^{-1}$ of ^{226}Ra and 2906 ± 262 $Bq.kg^{-1}$ of ^{228}Ra) and lead isotopes (960 ± 166 $Bq.kg^{-1}$ of ^{210}Pb). These values are higher than the concentrations present in the ilmenite mud studied by Llanes et al. [16], who observed concentrations of 520 ± 30 $Bq.kg^{-1}$ of ^{226}Ra and 2584 ± 2 $Bq.kg^{-1}$ of ^{228}Ra. Therefore, any application of this residue must be accompanied by a careful assessment of the radiation exposure.

The results obtained for $C_{Ra,eq}$ of mortars containing 5%, 10%, and 15% of the residue did not exceed the recommended value, which is up to 370 $Bq.kg^{-1}$, indicating that its use does not imply additional risks owing to external exposure. The results obtained for I were less than 1, ensuring that the dose of external gamma exposure from the mortar did

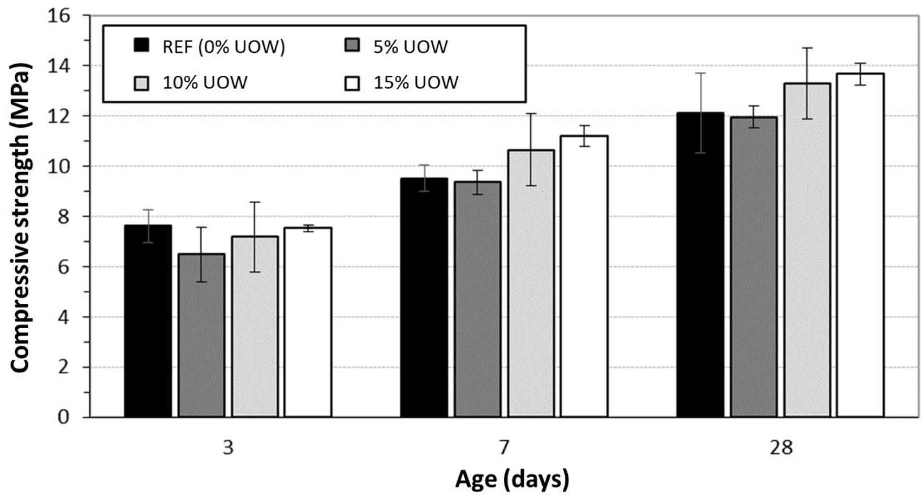

Fig. 10. Compressive strength of mortars with different levels of UOW, as a function of time.

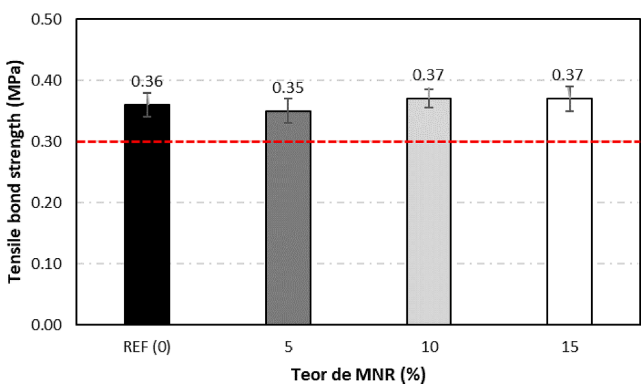

Fig. 11. Tensile bond strength of mortars, as a function of UOW content.

not exceed the value of 1 $mSv.a^{-1}$.

The Rn concentrations before and after the application of the coating mortar are listed in Table 7. The average concentration of radon in the standard room was 72 ± 11 $Bq.m^{-3}$ before mortar coating, which is of the same order of magnitude as the value determined after applying the mortar, compatible with the concentration of radon in the air in indoor environments and below the values recommended by the International Commission on Radiological Protection (ICRP) and the World Health Organization (WHO) of 300 and 100 $Bq.m^{-3}$, respectively. The external gamma exposure measured using a TLD was always less than 0.1 $mSv.a^{-1}$.

As UOW is an industrial waste, currently it has no commercial value, being currently paid for its disposal in landfills. Thus, industries that wish to use it in matrices to take advantage of its characteristics, such as the photocatalytic potential, have an advantage because its cost will hardly be higher than that of common materials used in this type of technology. It is only necessary to analyze issues of logistics and transport distance. Therefore, the investigation of life cycle analyzes and life cycle cost is strongly recommended, in order to verify the economic viability of this promising raw material.

4. Conclusions

The results obtained in this study indicate that unreacted ore waste (UOW) can be incorporated into cementitious matrices, presenting satisfactory results in accordance with the normative requirements imposed on coating mortars regarding their properties in the fresh, hardened, and applied states without presenting additional risks to users because of exposure to radiation. From the results obtained in this study, the following conclusions are drawn:

- The addition of UOW does not significantly impact the physical and mechanical properties of the coating mortar.
- The addition of UOW promotes significant reductions in mortar plasticity owing to the addition of fine particles. However, this effect can be reduced and/or avoided by adjusting the water/dry materials ratio and/or using superplasticizer admixtures.
- The addition of UOW does not significantly impact the tensile bond strength or low-pressure absorption of the coating mortar.
- The addition of UOW does not harm any fundamental property of the coating mortars and can be incorporated into the process, thereby replacing traditional raw materials.
- The addition of UOW to the coating mortars did not present any risk to the health of the users owing to exposure to external and internal gamma radiation and radon inhalation.

The addition of UOW in coating mortars allows the incorporation of this residue in a safe and technically satisfactory manner, without compromising on product quality, in addition to a reduction in the consumption of natural raw materials and making UOW a by-product.

CRediT authorship contribution statement

Daniel V. Ribeiro: Conceptualization, Funding acquisition, Supervision, Writing - review & editing. **Nilson S. Amorim:** Investigation, Methodology, Writing - review & editing. **José S. Andrade Neto:** Investigation, Methodology, Writing - review & editing. **Diana D.M. Albuquerque:** Investigation, Methodology, Writing - review & editing.

Table 5
ANOVA statistical analysis of results evaluating the influence of the addition of UOW on the properties of mortar on applied state.

Properties	Sum of squares	Degrees of freedom	Mean square	F value	P value	Fc critical	Significant effect
Tensile bond strength	0.00	3	0.00	0.82	0.5166	4.07	Not
Water absorption/permeability by the Karsten pipe	0.00	2	0.00	0.53	0.3257	4.07	Not

Note: If P less than 5%, and Fc < F value, the result is significant, considering the 95% confidence interval.

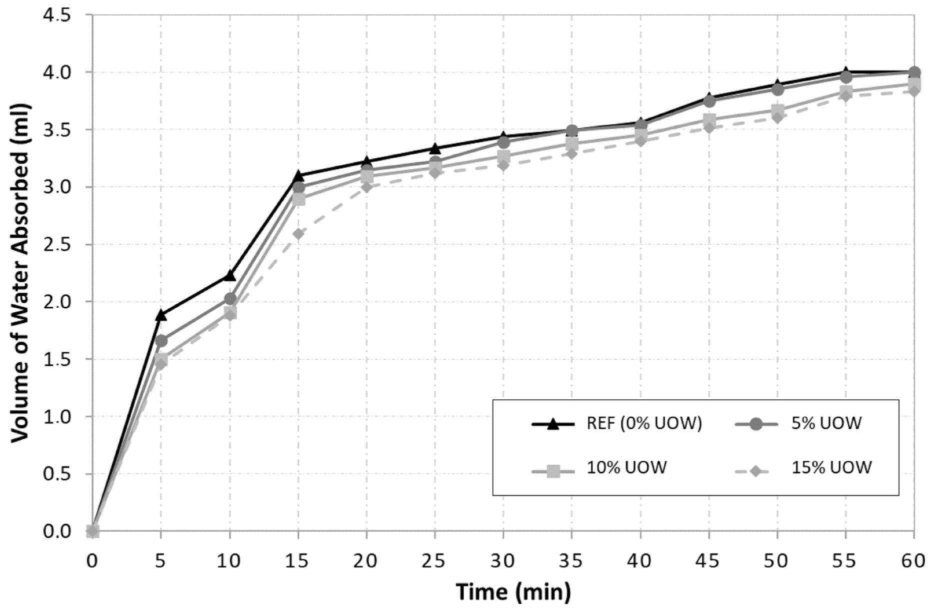

Fig. 12. Absorption of water under low pressure of the reference mortars and with additions of 5%, 10% and 15% of UOW, by the pipe method (Karsten Pipe) over 60 min.

Table 6
Average concentration of radionuclides in samples of UOW, lime, sand, cement and mortar with different proportions of UOW (Bq.kg^{-1}), Radium Equivalent Activity ($C_{Ra,eq}$, Bq kg^{-1}) and Activity Concentration Index (I) of mortars.

Sample	U-238	Ra-226	Pb-210	Th-232	Ra-228	K-40	Ra_{eq}	I
UOW	538 ± 103	1103 ± 115	960 ± 166	400 ± 82	2906 ± 262	119 ± 50		
lime	10 ± 3	11 ± 1	10 ± 1	1.7 ± 0.2	5.2 ± 0.4	22 ± 4		
sand	8.6 ± 3.2	3.3 ± 0.7	5.0 ± 1.1	2.6 ± 1.0	2.4 ± 0.5	15 ± 9		
cement	39 ± 9	50 ± 3	54 ± 14	14 ± 3	12 ± 2	215 ± 28		
5% UOW	17 ± 4	19 ± 1	15 ± 3	12 ± 3	26 ± 2	11 ± 2	37	0.13
10% UOW	21 ± 2	26 ± 2	19 ± 5	15 ± 7	45 ± 3	15 ± 6	49	0.17
15% UOW	24 ± 4	33 ± 2	24 ± 4	18 ± 5	66 ± 5	16 ± 6	60	0.20

Table 7
Concentration of radon (Rn) in the air before and after applying the mortar (Bq. m^{-3}).

Sampling location	Rn Before application	Rn After application
Center of the room	74.4 ± 3.3	63.0 ± 4.9
Behind the entrance door	84.5 ± 3.8	105.3 ± 8.2
Room background	58.6 ± 2.6	44.3 ± 3.4
Average	72 ± 11	71 ± 25
External	56.1 ± 2.5	13.5 ± 1.1

Barbara P. Mazzilli: Investigation, Methodology, Writing - review & editing.

Declaration of Competing Interest

The authors declare that they have no known competing financial interests or personal relationships that could have appeared to influence the work reported in this paper.

Acknowledgments

The authors would like to thank FAPESB - Fundação de Amparo à Pesquisa do Estado da Bahia, CNPq - Conselho Nacional de Desenvolvimento Científico e Tecnológico (for research grants 300835/95-7 and 301133/2018-2), CAPES - Coordenação de Aperfeiçoamento de Pessoal de Nível Superior and TRONOX Pigmentos do Brasil.

References

[1] ASSOCIAÇÃO BRASILEIRA DE EMPRESAS DE TRATAMENTO DE RESÍDUOS (ABETRE). Panorama dos resíduos sólidos do Brasil. 2016. Disponível em: <http://abrelpe.org.br/panorama/>. Acesso em 02 de fevereiro de 2021.
[2] S. Luhar, I. Luhar, Potential application of E-wastes in construction industry: a review, Constr. Build. Mater. 203 (2019) 222–240.
[3] M. Smol, J. Kulczycka, A. Henclik, K. Gorazda, Z. Wzorek, The possible use of sewage sludge ash (SSA) in the construction industry as a way towards a circular economy, J. Clean. Prod. 95 (2015) 45–54.
[4] S.C. MOGHADDAM, R. MADANDOUST, M. JAMSHIDI, I.M. NIKBIN. Mechanical properties of fly ash-based geopolymer concrete with crumb rubber and steel fiber under ambient and sulfuric acid conditions, Constr. Build. Mater. 281(122571) 2021.
[5] S. LUHAR, T.W. CHENG, I. LUHAR. Incorporation of natural waste from agricultural and aquacultural farming as supplementary materials with green concrete: a review, Compos. Part B: Eng. 175(107076) 2019.
[6] S. Luhar, S. Chaudhary, I. Luhar, Development of rubberized geopolymer concrete: Strength and durability studies, Constr. Build. Mater. 204 (2019) 740–753.
[7] D.V. Ribeiro, A.S. Silva, J.A. Labrincha, M.R. Morelli, Rheological properties and hydration behavior of Portland cement mortars containing calcined red mud, Can. J. Civ. Eng. 40 (6) (2013) 557–566.
[8] R.V. Silva, J. de Brito, R.K. Dhir, Performance of cementitious renderings and masonry mortars containing recycled aggregates from construction and demolition wastes, Constr. Build. Mater. 105 (2016) 400–415.
[9] A. Arora, U. Dave, Utilization of E-waste and plastic bottle waste in concrete, Int. J. Stud. Res. Technol. Manage. 1 (2013) 398–406.
[10] M.N.N. KHAN, P.K. SARKER. Effect of waste glass fine aggregate on the strength, durability and high temperature resistance of alkali-activated fly ash and GGBFS blended mortar. Constr. Build. Mater. 263(120177) 2020 12.
[11] M. SAMADI, G.F. HUSEIEN, H. MOHAMMADHOSSEINI, H.S. LEE, N.H.A.S. LIM, M.M. TAHIR, R. ALYOUSEF. Waste ceramic as low cost and eco-friendly materials in the production of sustainable mortars, J. Clean. Prod. 266(121825) 2020 17.
[12] M. Zalas, A. Cynarzewska, Application of paper industry waste materials containing TiO2 for dye-sensitized solar cells fabrication, Optik 158 (2018) 469–476.
[13] AD.D.M. LBUQUERQUE, N.S. AMORIM JÚNIOR, V.S. SANTOS, D.V. RIBEIRO. Avaliação das propriedades físicas e da capacidade fotocatalítica das argamassas contendo resíduo proveniente da produção do dióxido de titânio (MNR). In: anais do XII Simpósio Brasileiro de Tecnologia das Argamassas (SBTA), São Paulo, Brazil, p. 1-11, 2017.

[14] T.R.S. Nobre, T.A. Santos, J. Alves, D.V. Ribeiro, Efeito da adição do resíduo proveniente do beneficiamento de TiO2 em pastas cimentícias: análise pela técnica de DRX, Anais do VIII Encontro Científico de Física Aplicada, Vitória, Brazil, 2017.
[15] J. da Silva Andrade Neto, D.D.M. de Albuquerque, N.S. Amorim Júnior, D. V. Ribeiro, Effect of the addition of unreacted ilmenite (UOW) on the hydration of white portland cement - hydrated lime pastes, Key Eng. Mater. 803 (2019) 289–293.
[16] M.C. Llanes, M.J.G. González, S.M.P. Moreno, J.P.B. Raya, Recovery of ilmenite mud as an additive in commercial Portland cements, Environ. Sci. Pollut. Res. 25 (2018) 24695–24703.
[17] J.H. POTGIETER, K.A. HORNE, K.A. POTGIETER, W. WIRTH. An evaluation of the incorporation of a titanium dioxide producer's waste material in Portland cement clinker, Mater. Lett. 57(1) 2002 157-16.
[18] J.S. ANDRADE NETO, B.B. MARIANI, N.S. AMORIM JUNIOR, D.V. RIBEIRO, Characterization of Cements Produced from Clinker Co-Processed with TiO2 Waste (UOW), Key Eng. Mater. 803 (2019) 278–283.
[19] B.B. MARIANI, J.S. ANDRADE NETO, N.S. AMORIM JÚNIOR, D.V. RIBEIRO. Ambiente Construído 19 2019 57-71.
[20] G.S. McNULTY. Production of titanium dioxide, in: Proceedings of NORM V International Conference, Seville, Spain, p. 169–189, 2007.
[21] D.D.M. de Albuquerque, J.S. Andrade Neto, N.S. Amorim Júnior, V.S. Santos, D. V. Ribeiro, Evaluation of the Influence of the Waste Originated by the Production of Titanium Dioxide (URM) on the Physical-Mechanical Properties of Coating Mortars, Key Eng. Mater. 765 (2018) 319–323.
[22] M.J. Gázquez, J. Mantero, J.P. Bolívar, R. García-Tenorio, F. Vaca, R.L. Lozano, Physico-chemical and radioactive characterization of TiO2 undissolved mud for its valorization, J. Hazard. Mater. 191 (1-3) (2011) 269–276.
[23] ASSOCIAÇÃO BRASILEIRA DE NORMAS TÉCNICAS (ABNT). NBR 10007 - Sampling of solid waste (in portuguese). Rio de Janeiro, 2004.
[24] W.J. SANTOS. Desenvolvimento de metodologia de dosagem de argamassas de revestimento e assentamento. Dissertação de Mestrado, Programa de Pós-Graduação em Engenharia Civil. Universidade Federal de Viçosa, Viçosa, Brasil, 2014.
[25] ASSOCIAÇÃO BRASILEIRA DE NORMAS TÉCNICAS (ABNT). NBR 13276 - M ortars applied on walls and ceilings - Determination of the consistence index (in portuguese). Rio de Janeiro, 2016.
[26] ASSOCIAÇÃO BRASILEIRA DE NORMAS TÉCNICAS (ABNT). NBR NM 248 – Aggregates - Sieve analysis of fine and coarse aggregates (in portuguese). Rio de Janeiro, 2003.
[27] ASSOCIAÇÃO BRASILEIRA DE NORMAS TÉCNICAS (ABNT). NBR NM 52 - Fine aggregate - Determination of the bulk specific gravity and apparent specific gravity (in portuguese). Rio de Janeiro, 2009.
[28] P.F.G. Banfill, Rheological methods for assessing the flow properties of mortar and related materials, Constr. Build. Mater. 8 (1) (1994) 43–50.
[29] F.A. Cardoso, V.M. John, R.G. Pileggi, Rheological behavior of mortars under different squeezing rates, Cem. Concr. Res. 39 (9) (2009) 748–753.
[30] ASSOCIAÇÃO BRASILEIRA DE NORMAS TÉCNICAS (ABNT). NBR 15839 - Rendering mortar for walls and ceilings - Rheological evaluation by squeeze-flow (in portuguese). Rio de Janeiro, 2010.
[31] ASSOCIAÇÃO BRASILEIRA DE NORMAS TÉCNICAS (ABNT). NBR 13279 – Mortars applied on walls and ceilings - Determination of the flexural and the compressive strength in the hardened stage (in portuguese). Rio de Janeiro, 2005.
[32] ASSOCIAÇÃO BRASILEIRA DE NORMAS TÉCNICAS (ABNT). NBR 9778 – Hardened mortar and concrete - Determination of absorption, voids and specific gravity (in portuguese). Rio de Janeiro, 2005.
[33] ASSOCIAÇÃO BRASILEIRA DE NORMAS TÉCNICAS (ABNT). NBR 15630 – Mortars applied on walls and ceilings - Determination of elasticity modulus by the ultrasonic wave propagation (in portuguese). Rio de Janeiro, 2008.
[34] ASSOCIAÇÃO BRASILEIRA DE NORMAS TÉCNICAS (ABNT). NBR 13528 – Render made of inorganic mortars applied on walls - Determination of bond tensile bond strength (in portuguese). Rio de Janeiro, 2010.
[35] Centre Scientifique et Technique de la Construccion – CSTC 140. Hidrofuges de surface: choix et mise en oeuvre. Bruxelles, 24 p. (Note D'information Technique – NIT n. 140), 1982.
[36] European Commission – Radiation protection 112. Radiological Protection Principles concerning the Natural Radioactivity of Building Materials, 16 p., 1999.
[37] A.I. LASKAR. Correlating slump, slump flow, vebe and flow tests to rheological parameters of high-performance concrete. Mater. Res. 12(1) 2009 75-81.
[38] R.I. OLIVEIRA, A.R. STUDART, R.G. PILEGGI, V.C. PANDOLFELLI. Dispersão e Empacotamento de Partículas. Princípios e aplicações em processamento cerâmico, Fazendo Arte Editorial, São Paulo, Brasil, 195 p., 2000.
[39] M. Yang, H.M. Jennings, Influences of mixing methods on the microstructure and rheological behavior of cement paste, Adv. Cem. Based Mater. 2 (2) (1995) 70–78.
[40] L.D.O. HADDAD, R.R. NEVES, P.V. OLIVEIRA, W.J. SANTOS, J.R. CARVALHO, A. N., W.J. SANTOS. Influence of particle shape and size distribution on coating mortar properties. J. Mater. Res. and Technol., v. 9, i. 4, p. 9299-9314, 2020.
[41] G.A. Silva Neto, M.B. Leite, Study of the influence of the mortar fine recycled aggregate ratio and the mixing sequence on the behavior of new mortars, Ambiente Construído 18 (2) (2018) 53–69.
[42] S.H. BEHRENS. Oil-coated bubbles in particle suspensions, capillary foams, and related opportunities in colloidal multiphase systems. Curr. Opin. Colloid Interface Sci. v. xx, in press, 2020.
[43] R.G. Pileggi, A.R. Studart, J. Gallo, V.C. Pandolfelli, How mixing affects the rheology of refractory castables - Part II, Am. Ceram. Soc. Bull. 80 (2001) 27–31.
[44] A.L.de. Castro, J.B.L. Liborio, V.C. Pandolfelli, Reologia de concretos de alto desempenho aplicados na construção civil – Revisão, Cerâmica 57 (341) (2011) 63–75.
[45] G. Skripkiūnas, D. Nagrockienė, G. Girskas, M. Vaicienė, E. Baranauskaitė, The cement type effect on freeze – thaw and deicing salt resistance of concrete, Procedia Eng. 57 (2013) 1045–1051.
[46] Y. Benachour, C.A. Davy, F. Skoczylas, H. Houari, Effect of a high calcite *filler* addition upon microstructural, mechanical, shrinkage and transport properties of a mortar, Cem. Concr. Res. 38 (6) (2008) 727–736.
[47] L.A. Dias, H. Carasek, Avaliação da permeabilidade e da absorção de água de revestimentos de argamassa pelo método do cachimbo, in: V Simpósio Brasileiro de Tecnologia das Argamassas, São Paulo, 2003, pp. 519–532.